Determination of the Response Characteristics of the Atomlab Re-entrant Ionization Chamber

by
David Courtney Rayburn

A thesis submitted to the
Florida Institute of Technology
in partial fulfillment of the requirements
for the degree of

Master of Science
in
Physics

Melbourne, Florida

April, 2007

We the undersigned committee
hereby approve the attached thesis

"Determination of the Response Characteristics
of the Atomlab Reentrant Ionization chamber"
by
David Courtney Rayburn

Laszlo Baksay, Ph.D
Professor, Physics

William W. Arrasmith, Ph.D.
Associate Professor
Engineering Systems

Marcus Hohlmann, Ph.D.
Assistant Professor, Physics

William Simon, M.S.
President
Sun Nuclear Corporation

Terry D. Oswalt, Ph.D.
Department Head, Physics and Space Sciences

Abstract

Title: Determination of the Response Characteristics of the Atomlab Re-entrant Ionization Chamber

Author: David Courtney Rayburn

Principal Advisor: Laszlo Baksay, Ph. D.

The photon energy response curve of the Atomlab dose calibrator ionization chamber is determined. The response is measured for select gamma and positron emitting radioisotopes. Analysis of the data points generated from select isotopes is used to correct a Monte-Carlo model of the ionization chamber, in order to determine the response curve.

Table of Contents

List of Figures

List of Tables

Acknowledgments

I would like to thank the following people for all the help and support that they have given me during this project:

Bill Simon - for giving me the opportunity to work on this thesis at Sun Nuclear Corporation, and for providing excellent guidance and knowledge on the subject.

Jakub Kozelka - for his help with the Monte Carlo simulation of the Atomlab response curve, and for many great discussions about science.

Laszlo Baksay – for his guidance in the thesis process and his academic support throughout my graduate school experience.

Marcus Hohlmann – for being nice and taking the time to be on my committee.

William Arrasmith – for his help and guidance with other projects, and also for taking the time to be on my committee.

Kimberley Hargrove – for loving me and supporting me through everything.

Introduction and Background

A dose calibrator is an instrument which is used to measure the radiopharmaceutical dose which is given to a medical patient. The radiopharmaceutical dose may be given for treatment, as a palliative, or it may be used for imaging purposes. The dose may be measured in the dose calibrator at a pharmacy or cyclotron facility, and it is often measured again at the point-of-use (a clinic or hospital) to verify the dose before administration to a patient.

Accuracy is important to measurement of radiopharmaceutical doses in order to deliver the medically prescribed dose of radiopharmaceutical to the patient. A dose which is too large will result in the patient receiving more radiation than necessary (a violation of the ALARA "As Low As Reasonably Achievable" radiation safety principle), or even a harmful or fatal dose. A dose which is too small may be ineffective for its intended purpose.

The Atomlab dose calibrator is one of the two most commonly used dose calibrators in the world, with the other one being the Capintec CRC line of chambers. The primary difference between the Atomlab and Capintec chambers is the shape of the axial response curve, with the Capintec having its flattest response in the middle of the well, and the Atomlab having its flattest response near the

bottom of the well. This area of small change in radiation sensitivity with respect to position is often referred to as a chamber's "sweet spot".

Ionization chambers

A dose calibrator uses a type of radiation detector called a re-entrant ionization chamber. An ionization chamber is a type of gas-filled detector which operates with a voltage differential below that of a proportional counter. In a gas-filled detector, ions and free electrons are created in the gas by the passage of ionizing radiation. The voltage differential between the cathode and anode causes the ions and electrons to drift towards the cathode and anode respectively. Unsealed air filled chambers can be used, but argon is more commonly used in re-entrant ionization chambers due to its low electron attachment coefficient, inertness, and ionization potential. A re-entrant ionization chamber (refer to Figure 1, following page) is an ionization chamber that forms a cylindrical well into which doses of radionuclides can be placed for measurement one at a time, and then removed. Placement of the source in the well results in an almost 4π steradian angular coverage, completely surrounding the radiation source.

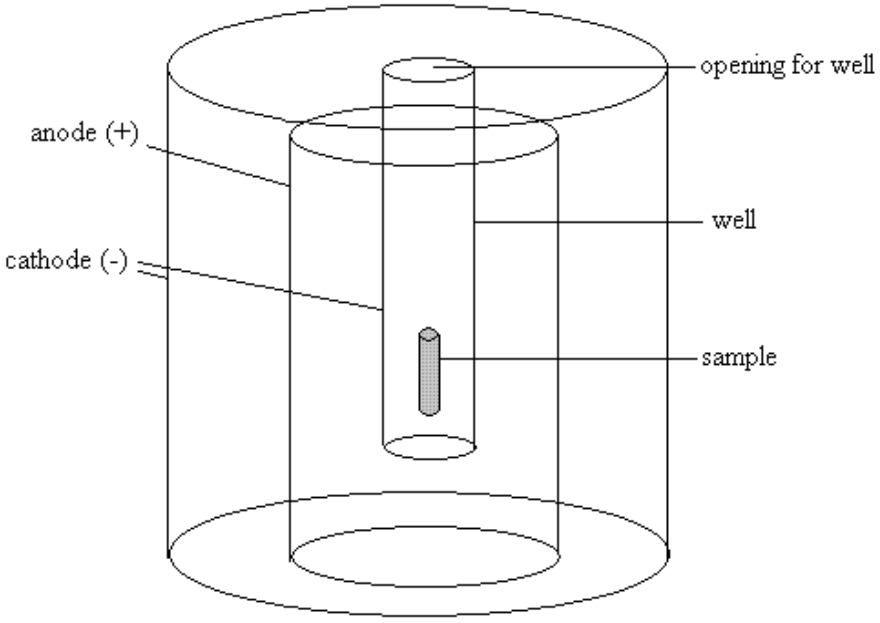

Figure 1: Re-entrant Ionization Chamber Diagram

The number of free electrons and positive ions which are produced by the passage of radiation through the detector gas is proportional to the amount of energy deposited by the radiation, and inversely proportional to the amount of energy that is required, on average, to create a free electron and positive ion. The amount of energy which is required to create an ion-electron pair is called *W*. The ionization energy of the least bound electron in argon is only 15.75 eV. However, not all energy from the radiation will be used in ionizing argon atoms. Some part of the energy will be absorbed in excitation processes that do not result in ionization. Because of this, *W* is always greater than the ionization energy of the weakest

bound electron. In argon, *W* has been measured to be 26.4 to 27.0 eV per ion-electron pair.[1,2]

If the voltage gradient is too large for a given gas density, then a multiplication process called a Townsend avalanche occurs, with mobile electrons and ions striking neutral gas atoms with enough energy to ionize them[2]. The newly generated ions and electrons then also gain energy from the electric field, and move towards the cathode and anode. This results in multiplication of the current within the gaseous detector. At voltage gradients above those used in ionization chambers, the amount of current produced is proportional to the amount of ionization produced by the radiation. This is referred to as the proportional regime. At voltage gradients above the proportional regime, the multiplication occurs so quickly that a discharge occurs and the voltage differential cannot be maintained. That is the basis of a Geiger-Muller counter. In the ionization chambers used in dose calibrators, Townsend multiplication is not a significant factor.

Recombination of the ions within the gas volume can be a significant factor however. The rate of ion recombination is largely determined by the impurities within the argon gas. Gases with a high electron attachment coefficient such as O_2 and H_2O can combine with mobile free electrons, creating negative ions. The drift velocity of negative ions is three orders of magnitude lower than that of free

electrons, because of the higher mass of the negative ion relative to the free electron. Due to the applied voltage, the free electrons are able to be collected from the chamber fast enough that they have a low chance of recombining with the positive ions in the chamber. However, negative ions move slowly enough that there is a significant chance that a positive and negative ion will recombine, causing a portion of the chamber's current to be lost. Recombination is a significant factor when the chamber gas has a significant portion of electronegative gas.

The current generated by a chamber per given amount of radionuclide is termed its response. The response of the chamber varies for different radionuclides, as different isotopes have different distributions of particle energies. For example, in the original Atomlab dose calibrator, 5 milliCuries of Co-60 will generate the same amount of current as 33.6 milliCuries of Tc-99m. Because of this, a conversion factor or "dial value" is generally provided for each isotope, which converts the measured current to the correct displayed activity for the isotope being measured. Ionization chambers do not have the ability to determine which isotope is being measured, so the user must select the correct dial value for the isotope. In addition, each chamber will usually have a calibration factor, which is the measured response for a calibration isotope. Calibration isotopes are usually chosen to have long half-

lives for stability of readings and relatively high energy gamma emissions in order to avoid difficulties with measurement of low energy particles (see below). The Atomlab dose calibrator uses Co-60 as its calibration isotope.

Measurement of low energy (<70 keV) gammas and beta radiation of any energy exhibits additional difficulties. All radioisotope alpha particles, as well as beta particles below an energy of approximately 1.5 MeV, will not penetrate the aluminum wall of the ionization chamber to deposit energy in the argon gas. Negative beta particles (electrons) can only be detected by the bremsstrahlung emitted from their energy loss in the aluminum. This bremsstrahlung consists of low energy photons. Alpha particles cannot be detected at all by re-entrant ionization chambers at the energies emitted from radioisotopes.

The measurement of low energy photons is complicated by their high attenuation coefficients in matter. This means that the container and/or solution used to hold the radiopharmaceutical has a significant effect upon the measurement. For example, consider the difference in effect of traversing 1 mm of PMMA (polymethyl methacrylate) plastic upon a 1 MeV photon and a 30 keV photon. The mass attenuation coefficient[10] for 1 MeV is $(\mu/\rho) = 6.87 \times 10^{-2}$ cm^2/g and the mass attenuation coefficient for 30 keV is $(\mu/\rho) = 3.032 \times 10^{-1}$ cm^2/g. A 1 mm thickness of PMMA has a mass of 0.119 g/cm^2. Using the mass attenuation equation:

$$I / I_0 = \exp[-(\mu / \rho) \cdot x]$$

where I is the intensity, I_0 is the original intensity, (μ/ρ) is the mass attenuation coefficient, and x is the areal mass density; the difference in intensity between 30 keV photons and 1 MeV photons resulting from 1 mm of travel through PMMA plastic is 3.5%.

This high effect of attenuation in small thicknesses of matter for low energy photons and electrons means that an additional correction factor or factors must be used when measuring low energy gamma emitters or beta emitters. Extreme care must be taken to ensure that measurement geometries, including syringe or vial type, syringe holder, volume filling, and dipper and liner type, remain constant so that the proper correction factor can be used[5,14]. Not applying a correction factor of this type to low energy gamma measurements is a common source of error [5].

Changes to the Atomlab Chamber

The Atomlab chamber has been manufactured by Sun Nuclear Corporation (SNC) as a private label for Biodex Medical Systems, Inc. since 1991. In this time, no design changes have been made to either the chamber or the electrometer which have changed the response curve. However, a new chamber is now being manufactured by Sun Nuclear with some changes which have a significant effect upon the chamber's response curve.

In order to more easily comply with USDOT (United States Department of Transportation) regulations on the shipment of pressurized gases, the argon pressure in the new Atomlab chamber was reduced from 90 psia (pounds per square inch absolute) to 38 psia. The mechanical dimensions (height, width, wall thickness, etc.) of the Atomlab chamber itself have remained the same. These mechanical dimensions are presented in Figure 2 on the following page. A change was also made to the o-ring seals in order to more securely seal the gas in the chamber. In addition, a new electrometer is being used to measure the ionization current of the chamber. A different lead shield is also being used.

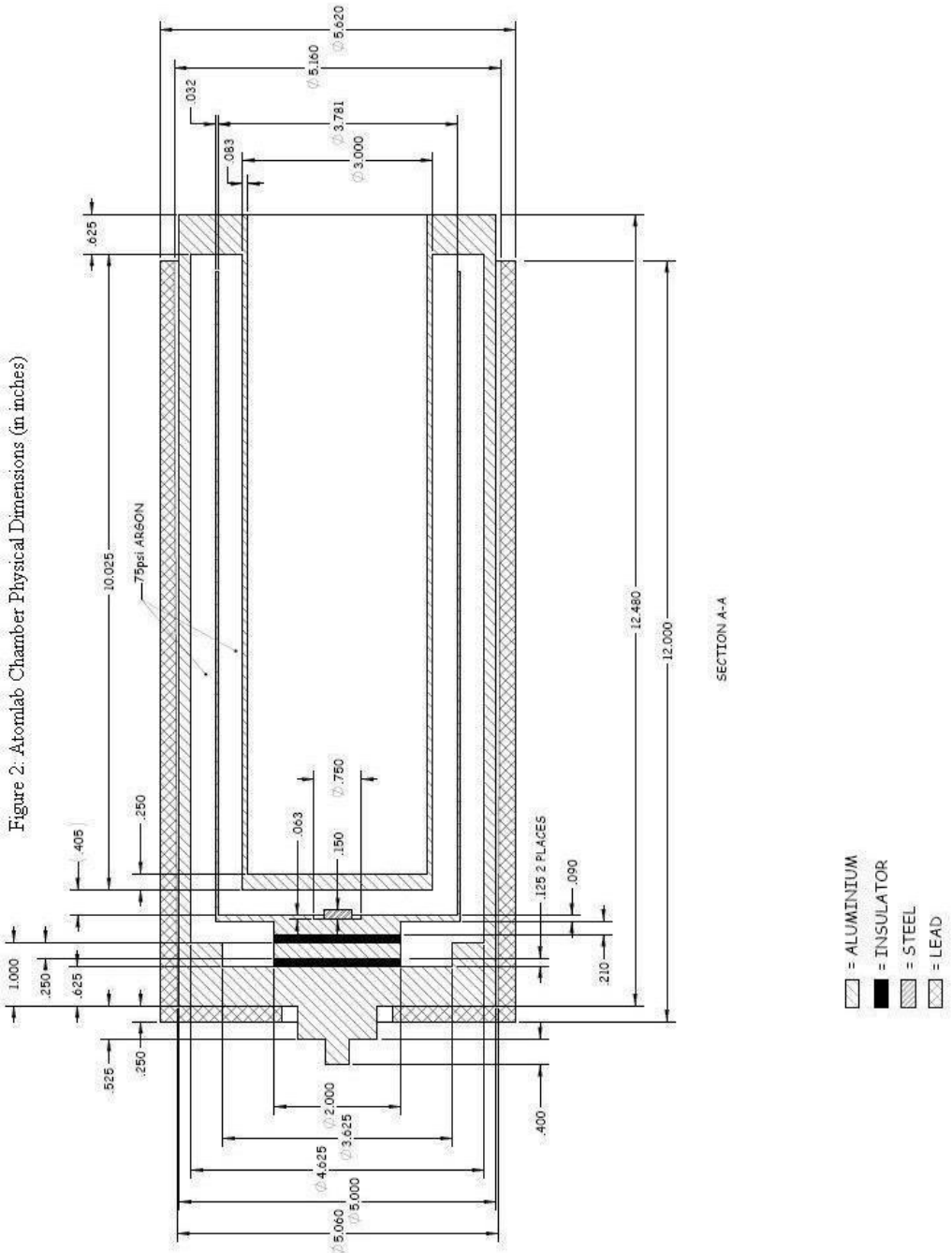

Figure 2: Atomlab Chamber Physical Dimensions (in inches)

The reduction in gas pressure (and thus density) is the most important factor affecting the response of the Atomlab chamber. The reduction in gas density is predicted to reduce the already low recombination rate, as gas volume ionic recombination is greater for higher pressures and higher proportions of electronegative gases. The gas mix and filling procedure remain the same: the chamber is filled with argon gas to a pressure of 75 psig (90 psia) 6 times before its pressure is set to 23 psig (38 psia). This ensures that the proportion of air remaining in the chamber is too small to cause appreciable ionic recombination effects. An estimate can be made of the amount of residual air in the chamber after this process, assuming that the chamber starts with 15 psia of air:

$$residual \quad air = \left(\frac{(15\,psia)\,Air}{(90\,psia)\,Argon} \right)^{6} = 2.14x10^{-5} = 0.00214\%$$

The reduction in gas density will also cause the overall calibration factor of the chambers to be different from the previous 75 psig chambers, as less gas means less ion-electron pairs for a radiation source of a given strength. The calibration factor is the ratio between the activity of the calibration isotope, Co-60 and the resultant chamber current. For the same gas mix, the chamber current for a given Co-60 activity is linear with respect to gas density. Thus, presuming the chambers are

filled at the same temperature, a new 23 psig (38 psia) chamber will have a calibration factor that is 90/38 of an old 75 psig (90 psia) chamber.

The reduction in gas density also has an effect upon the energy response curve. As the gas density is decreased, the response of the low energy photons increases relative to that of the higher energy photons. Unlike high energy photons, low energy photons deposit almost all of their energy in either the inner aluminum wall of the chamber, or in the argon gas. Of the energy deposited in the aluminum wall, some of it will cause secondary electrons to be emitted into the argon gas. The amount of secondary electrons is not related to the gas density, and as gas density is decreased, the relative effect of these secondary electrons will increase. Thus the response curve is expected to be higher in the low energy region for the newer low pressure chambers than it was in the older high pressure chambers.

The o-ring seal around the center connector of the Atomlab chamber has been altered to present a face-seal as opposed to the prior fit-seal. This is intended to reduce the amount of argon leakage out of the chamber. In addition, the o-ring gland seal between the chamber bottom and walls has been tightened, by reducing the groove depth by $5/1000^{th}$ of an inch. The tightening of the gland seal is to reduce gas leakage in cold environments.

A pressure sensor has also been added to the chamber to measure any significant change in pressure which occurs from a gas leak. A temperature sensor is also emplaced upon the chamber. The information from these sensors is read by a dedicated processor on the electrometer board. The combined pressure, temperature, and volume information allows for constant monitoring of the gas density inside the chamber. This monitoring enables the system to alert the user if a slow leak is detected, or when the gas density has fallen to such a point that the chamber needs to be recalibrated.

The new electrometer fits upon a single round circuit board, which is situated directly below the chamber. This is similar to the orientation in the original Atomlab chamber. A reduction in the size of electronic components over 20 years has made it possible to shrink the size of the electrometer board, so that the new board is about half the size of the old one. This has enabled the area which the chamber occupies to be reduced from an 18cm x 18cm square to a circle 15 cm in diameter.

Prior Response Data

The 90 psia ionization chamber response was characterized in 1991 by Simon[13]. Data points for the isotopes In-111, Xe-133, Tl-201, Tc-99m, I-123, Ba-133, I-131, Cs-137 and Co-60 were measured, and plotted on a hand-drawn graph to generate the response curve of the 90 PSIA Atomlab ionization chamber (see figure 3 on following page). The response curve is normalized to Co-60 photons; as there are two Co-60 photons of an average energy of approximately 1200 keV, each one is given a normalized response of 0.5 (marked as point one on figure 3).

This response curve consists primarily of three features: the low energy rise and peak, the mid energy drop-off and lead peak influence, and the high energy Compton scattered absorption curve. Pair production can also occur above 1.02 MeV; however, it is not a dominant effect until photon energies are much higher than those of interest in dose calibrator isotopes.

Figure 3: Response Curve of the 90 Psia Chamber (Simon, 1991)

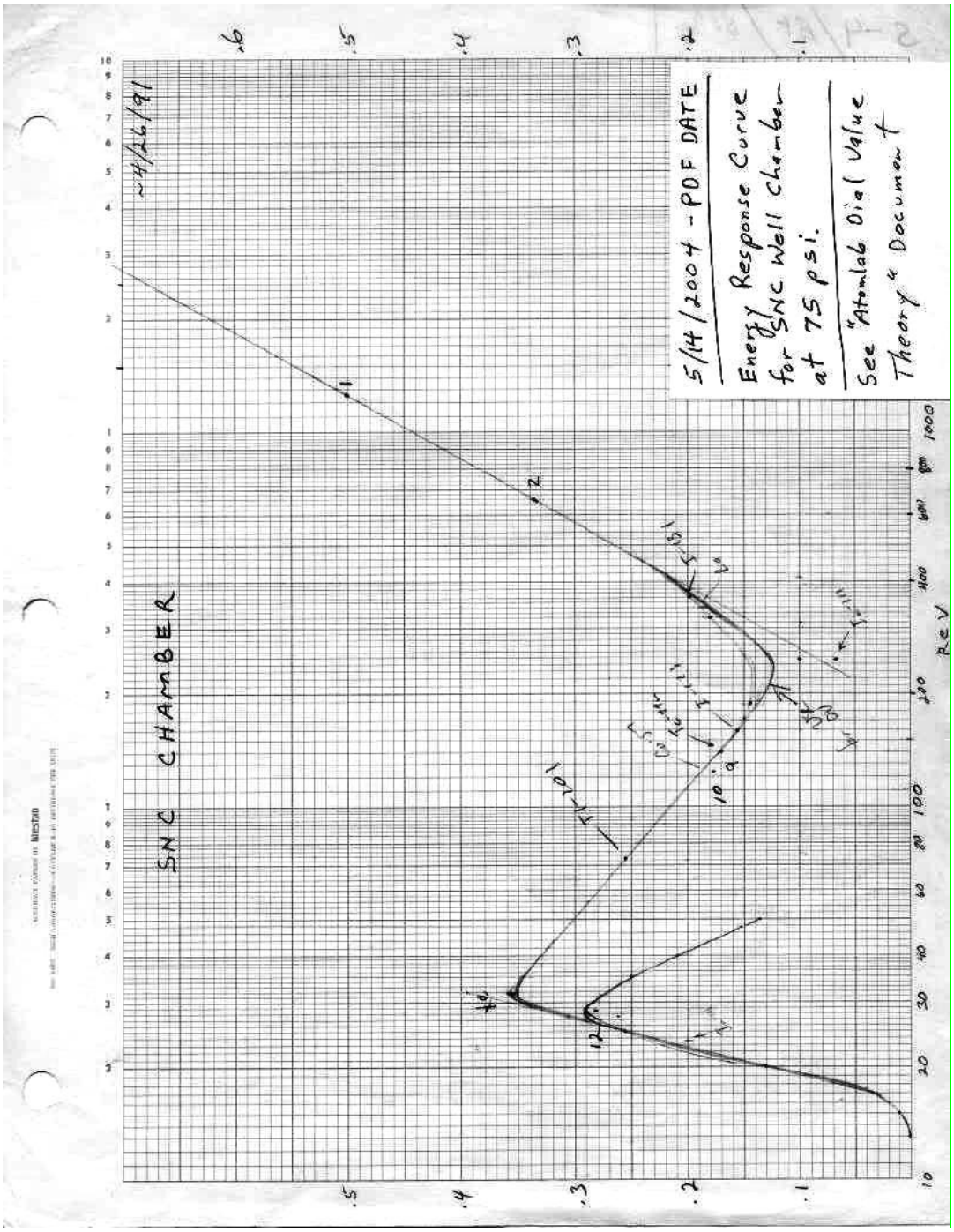

The low energy peak is a product of the photoelectric effect, combined with the attenuation effect of the aluminum wall. Low energy photons (<80 keV) can interact with atomic electrons, causing ionization of the atom. To cause a detectable response, ionization must occur within the argon gas. If no wall were present, the low energy response would match the mass attenuation coefficient μ/ρ of the argon gas itself, as presented in Figure 4.

Figure 4: Argon Mass Attenuation Coefficient as a Function of Photon Energy[10]

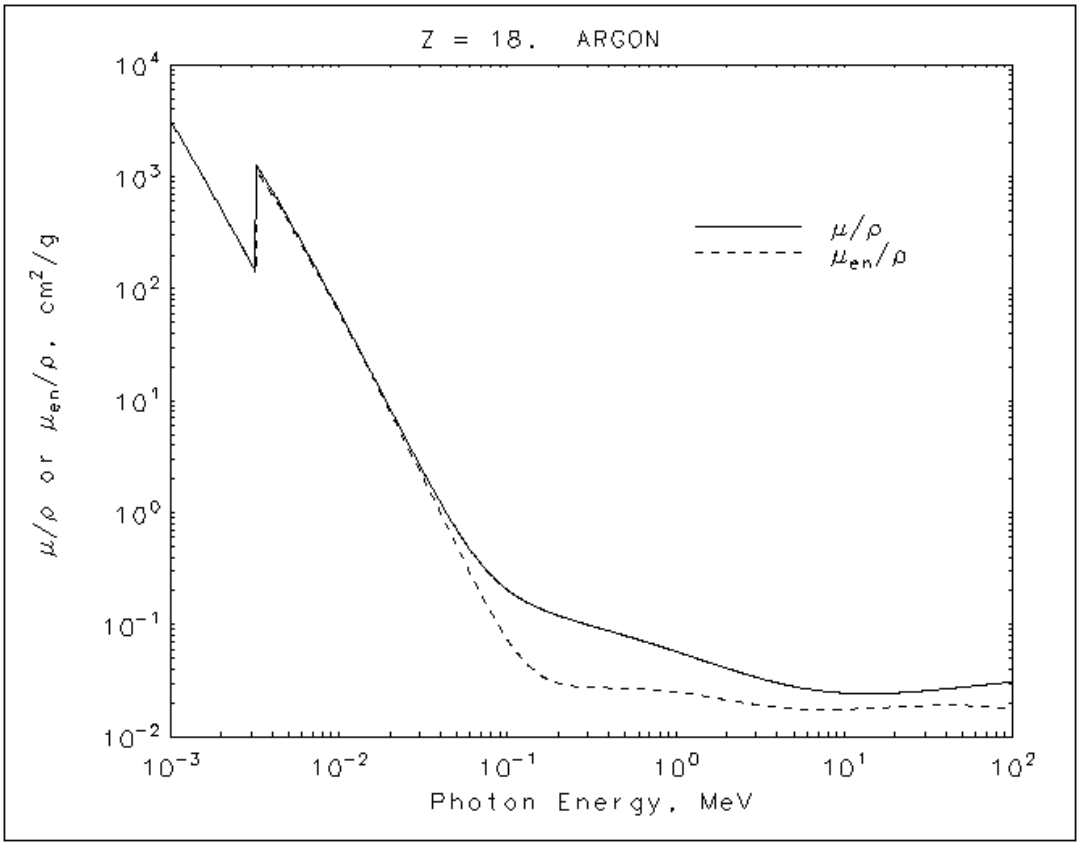

However, the attenuation of the low energy photons (below about 15 keV) within the aluminum wall means that the lowest energy portion of this curve does not contribute to the chamber response. The combination of the aluminum attenuation of low energy photons and the drop off in the photon attenuation in argon at higher energies causes the appearance of a peak in chamber response near the K-edge of argon.

A similar effect occurs in the range of photon energies above 88 keV. Photons are capable of backscattering off of the lead shielding which houses the chamber. Measurements with Co-57 using chambers which have the lead shields removed show a 22% increase in the response of the chambers when the lead shields are installed. This effect is referred to as the "Lead Peak", and it occurs due to photons of energy higher than 88 keV causing photons to be emitted from the lead back into the chamber. Note the discontinuity in the lead mass attenuation coefficient in Figure 5 at 0.088 MeV; this will appear later in the Monte Carlo modeling.

Figure 5: Lead Mass Attenuation Coefficient as a Function of Photon Energy[10]

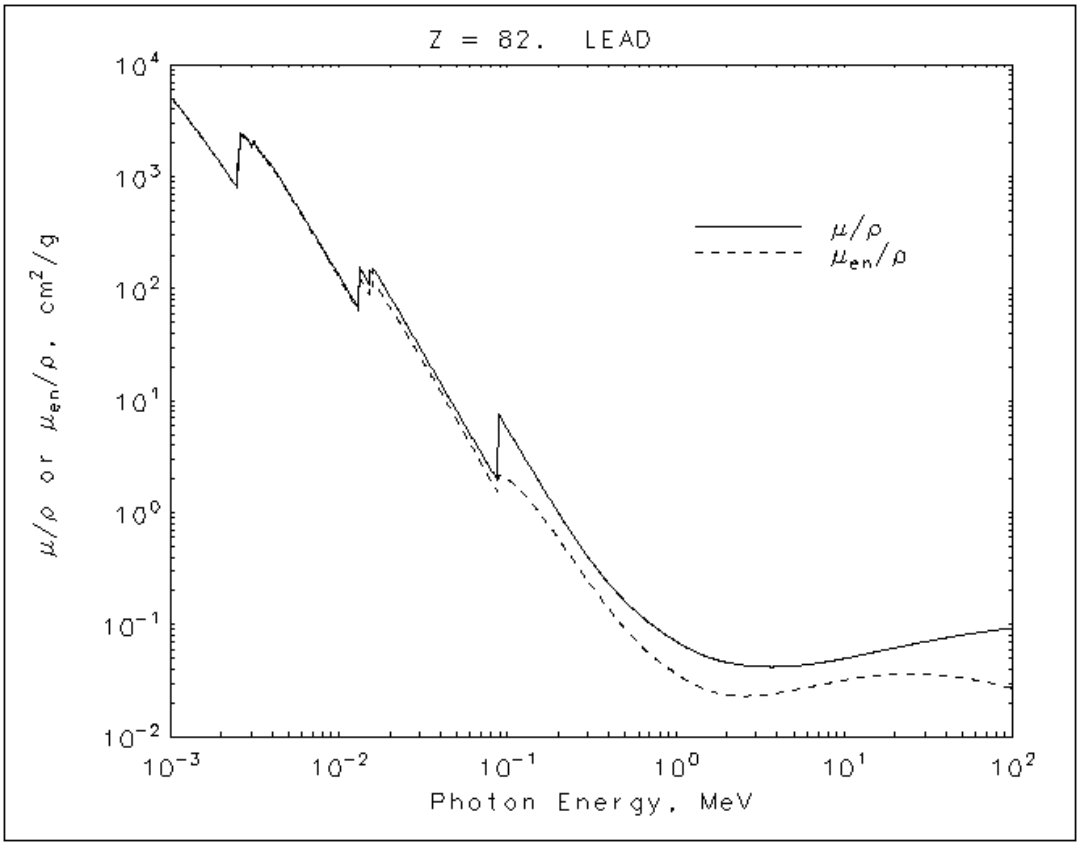

At higher photon energies, Compton scattering of photons is the main method of energy transfer from the photons to the argon gas. Compton scattering is the process of a photon deflecting off of an electron in the absorbing media. The electron which is involved in this scattering will recoil and absorb a fraction of the photon's energy. The recoil electron can create ion-electron pairs within the argon gas and be measured by the ion chamber. The probability of scattering is

proportional to the number of electrons in the absorbing material, and thus depends upon the electron density of the material.

In addition to photon response, beta radiation can also be measured by the dose calibrator. Alpha particles invariably deposit all of their energy in the aluminum skin of the chamber, or in the material which is used to surround the radioactive sample (such as water containing the radioisotope). As alpha particles do not generate bremsstrahlung, the alpha particles are not detectible. Beta particles (electrons or positrons) have the potential of entering the argon gas if their energy is high enough. The energy required for a particle to penetrate the chamber can be approximated from the Bethe-Bloch formula:

$$-\frac{dE}{dX} = \frac{4\pi}{m_e c^2} \cdot \frac{nz^2}{\beta^2} \cdot \left(\frac{e^2}{4\pi\varepsilon_0} \right)^2 \cdot \left[\ln\left(\frac{2m_e c^2 \beta^2}{I \cdot (1-\beta^2)} \right) - \beta^2 \right]$$

where E is the energy of the particle, X is the distance traveled, v is the instantaneous velocity of the particle, c is the speed of light, e is the charge of the electron, z is the charge of the particle (in units of e), m_e is the mass of an electron, n is the electron density of the medium, I is the mean excitation potential of the medium, and $\beta = v/c$.

However, the Bethe-Bloch formula provides a much better approximation for ions than for electrons[15]. Because of this, tables of measured stopping power provide a better estimate of the electrons' range in aluminum[16]. Simon's measurements from 1991 show no penetration for electrons with an energy of less than 1500 keV.

Due to this lower limit on penetrating particle energy, only the current from betas of 1500 keV or higher are including in calculations of chamber response. The chamber response from the penetrating betas has been measured to be approximately 4.9×10^{-6} of the response of an equal activity of Co-60 multiplied by the electron energy above 1500 in units of keV.

The bremsstrahlung produced by betas in the walls is much more detectable. This has been measured to be approximately 1.12x10-5 of the response of an equal activity of Co-60 multiplied by the electron energy in units of keV.

These electron response values were obtained by measurement of Y-90, a pure electron emitting isotope.[14]

Experimental Data

Sources and Geometries

In order to measure the response curve with respect to energy of the Atomlab chamber, measurements were made with a variety of NIST (National Institute of Standards and Technology) calibrated and NIST traceable radioisotope samples. The radiation produced by these samples was measured individually over the course of nearly a year.

Many of the isotopes that have been measured were provided by the NIST Standard Reference Materials program, which provides about 9 sources each year for nuclear medicine related applications. These NIST calibrated sources are used by nuclear medicine researchers and professionals as a standard amount of radioisotope which may be used for calibrating equipment, or for other purposes where a guaranteed known amount of isotope may be needed.

Nearly every month, a sample is shipped from the NIST to Sun Nuclear Corporation. Each sample is contained within a flame-sealed ampoule of borosilicate glass with a wall mass density of 0.134 g/cm^3. The sample is usually

composed of a salt of the radioisotope dissolved in 5 ml of saline water or weak acid. In the case of Xe-133, the ampoule contains a mix of Xe-133 gas and non-radioactive Xenon gas. The ampoule is 4.5 cm long, with a diameter of 1.5 cm, and a wall thickness of approximately 0.12 cm.

The Isotopes measured in this study are I-125, In-111, Tc-99m, Tl-201, Cs-137, Co-57, Ba-133, Co-60, I-131, Mo-99, Xe-133, F-18. This is a very similar list of isotopes to those used by Simon in 1991[13] to characterize the energy response curve of the original 75 psig chamber. The only isotopes measured which were not a NIST calibrated source were F-18, Co-60, Co-57, and Ba-133.

The Type E vial Cs-137 source (SNC 667-227-2) which was used in measurements was calibrated against a NIST calibrated Cs-137 source (SRM 4233C-42, calibrated 11/1/89). The Type E vial source was correct to within 0.5% of the NIST calibrated value.

Measurement Geometries

For NIST isotopes in ampoules, the ampoule was placed in a standing position in a standard Biodex source dipper. Each ampoule remained in its thin plastic bag covering, in case of breakage. The mass density of the plastic bag was very much

less than that of the borosilicate glass ampoule. A Biodex well liner was in the chamber. The clinical purpose of a well liner is to prevent spills from contaminating the chamber's well; it also adds additional attenuation to low-energy photons and betas, and thus it needs to be included in the measurement. The ampoule was then lowered in to the chamber, and a measurement was taken.

For sources in Type E vials, the vial was placed in a standing position in the bottom cup of a standard Biodex source dipper. A Biodex well liner was in the chamber. The vial was then lowered in to the chamber, and a measurement was taken.

For sources in syringes, the syringe was placed hanging in the syringe holder ring of the dipper. A Biodex well liner was in the chamber. The dipper was then lowered in to the chamber, and a measurement was taken.

Mo-99 was measured in a different manner than the other isotopes. Mo-99 is usually measured as a contaminant of Tc-99m samples, as Tc-99m is eluted from Mo-99 generators. There exists a regulatory standardized limit of 0.15 microCi Mo-99 per milliCi Tc-99m[6]. In order to separate the measurement of a Mo-99 contaminant from measurement of a sample of Tc-99m, a "Moly Breakthrough Shield" is used during measurement[12]. This is a lead container of thickness 6.4 mm that the sample is held in, within the ion chamber. This shield attenuates the lower

energy (~140 keV) Tc-99m photons, while allowing a portion of the higher energy (~740 keV) Mo-99 photons to be measured. Because this is the normal way in which this isotope is measured, the Mo-99 sample was measured with the NIST ampoule containing the Mo-99 sample inside of a Moly shield. The Moly shield was then placed in the well of the ion chamber, with a Biodex well liner in place.

Table 1: Measurement Geometry of Sources

Isotope	Geometry	NIST Calibrated?	NIST Traceable?
F-18	5 ml syringe	No	No
Co-57	Type E vial	No	Yes
Co-60	Type E vial	No	Yes
Tc-99m	Ampoule	Yes	Yes
Mo-99	Special	Yes	Yes
In-111	Ampoule	Yes	Yes
I-125	Ampoule	Yes	Yes
I-131	Ampoule	Yes	Yes
Ba-133	Type E vial	No	Yes
Xe-133	Ampoule	Yes	Yes
Cs-137	Type E vial	Special	Yes
Tl-201	Ampoule	Yes	Yes

Chambers

Three Atomlab 500 chambers were used for the primary measurements in this study. Their serial numbers are 4330802, 4330804, and 4330808. Each chamber has a calibration factor associated with it. The “calibration factor” is essentially a conversion factor which converts chamber current to Co-60 activity.

The calibration factor is determined during chamber calibration in the factory, by measuring the current produced in the chamber by a NIST traceable Co-60 source (source serial number MED 3550) with known activity and calculating the number of microcuries of Co-60 per picoampere. This calibration factor is stored in the chamber electronics for use in later measurements. The calibration factors stored in each chamber are listed in the below table:

Table 2: Chamber Calibration Factors (as stored, and to true precision)

SN	ID	Calibration Factor (as stored in electronics)	Calibration Factor (microcuries of Co-60/pA)
4330802	8	7.900826446	7.90
4330804	10	8.006700168	8.01
4330808	12	7.82964783	7.83

Although the calibration factors are stored with 16 bit precision, the actual accuracy of the 100 second measurements of chamber response to a 100 microCi Co-60 calibration source which the calibration factors is based upon is only good to within 0.2%. Thus for the remainder of this paper, all measurements will be truncated to 3 significant digit precision.

In addition, other chambers were used for measurement of variations in the wall thickness (and therefore low energy response) between chambers manufactured at different dates. These chambers, serial numbers 4633911, 4633905, 4633906, were manufactured a year later and in a different batch than the original three chambers.

Measurements

Photons

The following table lists the isotopes measured, along with the average measurement, and the response relative to Co-60. The error bars listed correspond to one standard deviation.

Table 3: Measured Isotope Response and Response Relative to Co-60

Isotope	Response (pA/microCi)	+/-	Response relative to Co-60	+/-
In-111	4.89E-02	1.1E-03	3.88E-01	8.6E-03
I-125	5.82E-02	1.5E-03	4.62E-01	1.2E-02
Xe-133	3.49E-02	3.5E-04	2.77E-01	2.8E-03
Tl-201	3.08E-02	6.2E-04	2.44E-01	4.9E-03
Co-57	1.87E-02	2.6E-04	1.49E-01	2.1E-03
Tc-99m	1.73E-02	2.6E-04	1.37E-01	2.0E-03
Ga-67	1.97E-02	3.4E-04	1.56E-01	2.7E-03
Ba-133	8.98E-02	2.0E-03	7.12E-01	1.5E-02
I-131	2.83E-02	7.9E-05	2.24E-01	6.2E-04
Cs-137	3.72E-02	5.2E-04	2.95E-01	4.1E-03
Mo-99	3.42E-03	3.0E-05	2.71E-02	2.4E-04
Co-60	1.26E-01	1.6E-03	1.00E+00	1.2E-02

In addition to the measurements listed above, the three more recent chambers were used to see if there might be a difference in wall thickness, and therefore low energy response, between the original group of chambers(SN 4330802, 4330804, and 4330808) and a more recently manufactured group (SN 4633911, 4633905, and 4633906).

It was determined using I-125 measurements that there existed a 12% average difference in the I-125 response relative to Co-60 between the more recent group and the original group of chambers. The more recent group had a much lower I-125 response relative to Co-60. Thus it is important to note that small differences in the chamber wall can have a significant effect upon low energy response.

Positrons

F-18 is the only positron emitting isotope which was measured as a part of this study. F-18 is the most commonly used positron isotope in positron emission tomography (PET) imaging, however it is not necessarily the best isotope for calibrating positron response. This is due to its short half-life (1.83 hours). Because of the short half-life, NIST calibrated F-18 samples were not available.

Ga-68 is a better isotope for calibration of positron response. Although it has a half-life of only 1.14 hours, it can be produced from a Ge-68 generator with a half-

life of 270.8 days. The generator can be calibrated, and thus the activity at a given time in the future would be known. Unfortunately, a generator of this type was not available for this testing. However, it should also be noted that Cs-137 has a primary photon of 661 keV, which is relatively close in energy to the 511 keV photon produced by electron-positron annihilation. The majority of the response from positrons comes from the photons produced by the electron-positron annihilation. Thus, Cs-137 provides a check on the portion of the response curve which applies to F-18 measurements.

Because a NIST standard was not available, F-18 was first measured in a set of 90 psia Atomlab chambers which have been established as a set of standard Atomlab 200 chambers. These chambers (serial numbers 38542032, 38542036, 38542046) have a continual record of response data going back to 2002, and their response is very well known. Mike Zimmer of Northwestern Memorial Hospital had previously measured a NIST calibrated sample of Ge-68/Ga-68 in a 90 psia Atomlab chamber with a 9.6 dial value and determined that it had an error of less than 2%.[7] Using these chambers with a dial value of 9.6 (the standard dial value for F-18 using 90 psia chambers) the activity of an F-18 source in 1 ml of fluid in a 5 ml syringe was measured. The syringe was then measured in the 3 standard 38 psia chambers. A Co-60 source of known activity was also measured in both kinds of

chambers. These measurements were time-corrected to the same time to account for the rather quick decay of F-18, and the relative response was calculated:

Table 4: Measured Positron Response and Response Relative to Co-60

Isotope	Response (pA/microCi)	+/-	Response relative to Co-60	+/-
F-18	6.84E-02	1.1E-03	5.42E-01	2.6E-02

Electrons

Unfortunately, due to circumstances beyond the author's control, an attempt to procure a NIST standard sample of Y-90 was unsuccessful. Thus, no measurement was made of any isotopes with pure or predominantly beta emission.

Monte Carlo Simulations of the energy response curve and their adjustments

Monte Carlo simulations can provide an accurate means of estimating the dose deposition of radiation into the ion chamber. Real ion chambers have a fairly complicated geometry. Because radiation can be absorbed, re-emitted and re-absorbed, a simulation of the absorption process can be more accurate than simply using the thickness of ion chamber elements as a guide to the energy response curve. However, real measurements must be used to validate or correct simulations of the energy response curve.

The energy response curve of the Atomlab chamber was also studied using PENELOPE Monte Carlo code[11]. The simulation uses the specified dimensions and materials of the Atomlab dose calibrator. The simulation sets the source position at the bottom of the dipper cup. The source is simulated as a point source, surrounded by a cylindrical body of water of radius 0.77 cm and height 2.81 cm, surrounded by a hollow borosilicate glass cylinder of the same radius and a height

of 3.8 cm, and of thickness 0.6 mm. This is intended to simulate the NIST ampoule.

Each isotope measured generates one or more gamma photons with each decay (F-18 generates positrons, which in turn generate 511 keV photons). In the appendix, table 8 shows the photon energies of each isotope measured, along with the probability of the photon emission with each decay[3,4]. Note that the photon energies below 200 keV are not shown for Mo-99, as these photon energies are attenuated by the Moly breakthrough shield during measurement. Table 9 also shows the spectrum of positron energies which are emitted from F-18.

The Monte Carlo calculation simulates the emission of photons at certain energies, and their resulting dose per photon of that energy in the chamber gas. It is this dose that contributes to the ionization of the gas, and hence to the ion current response of the chamber to the photon energy. From these discrete photon energies, a curve can be drawn which passes through the points created by each photon simulation. This curve can then be broken into sections that lend themselves to continuous fitting functions. This is demonstrated in Figure 6:

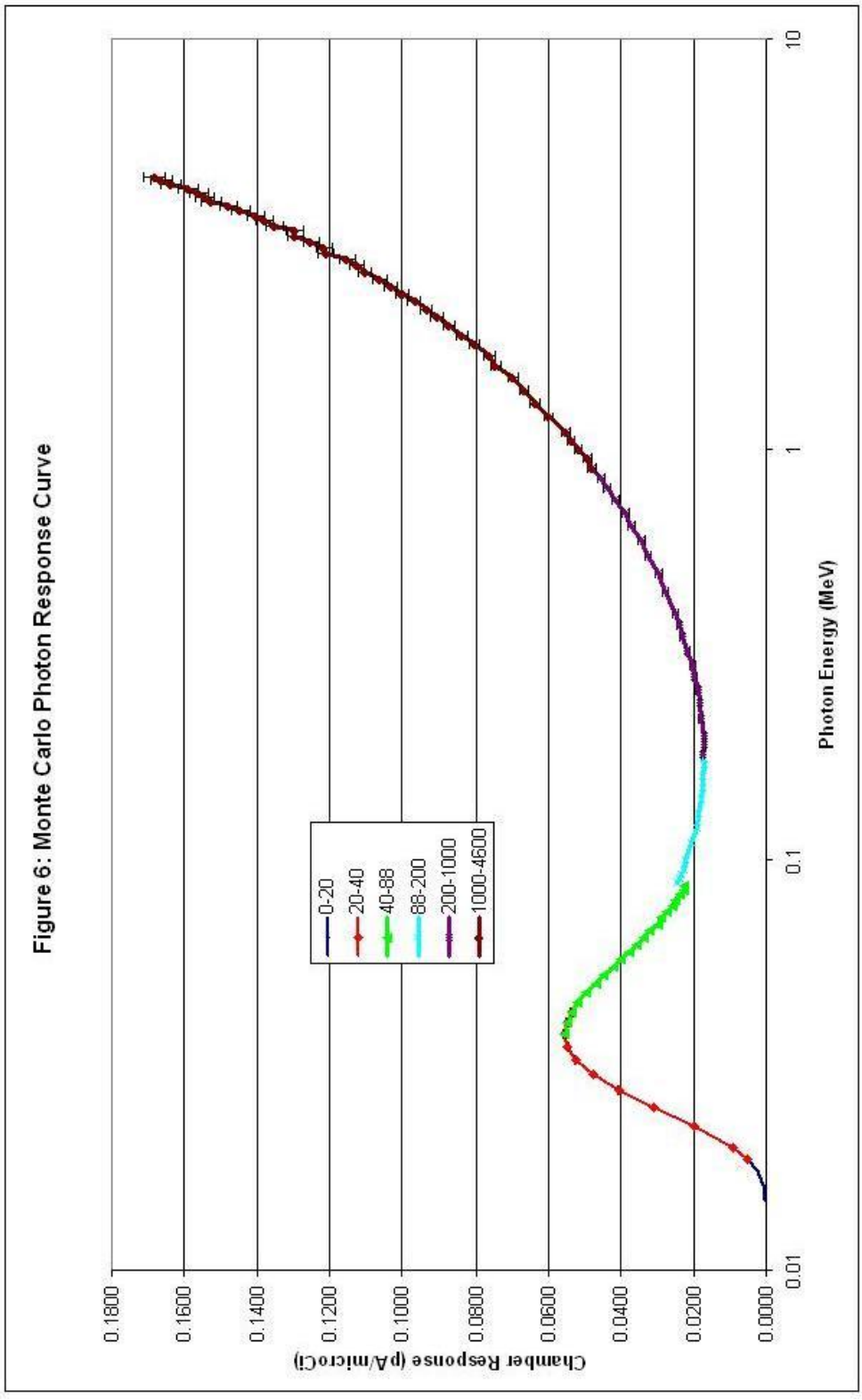
Figure 6: Monte Carlo Photon Response Curve
Chamber Response (pA/microCi)
0.1800
0.1600
0.1400
0.1200
0.1000
0.0800
0.0600
0.0400
0.0200
0.0000
0.01
0.1
1
10
Photon Energy (MeV)
0-20
20-40
40-88
88-200
200-1000
1000-4600

There is a statistical uncertainty to the Monte Carlo calculation which depends upon the number of particles simulated. This statistical uncertainty is noted upon the Monte Carlo chamber response curves with error bars which correspond to a 1 standard deviation error level. The error bars are too small to see on the graph at low energies.

Each section can be approximated closely using a fifth order polynomial. The polynomial function corresponding to each section of the energy response curve is recorded in the Appendix in Table 10: Monte Carlo Photon Response Curve Polynomial Expansion Coefficients.

From the fifth order polynomials, an estimate can be made of the relative response of the isotopes measured. By multiplying the appropriate coefficients by the given frequency of occurrence of each photon energy from Table 5 for each isotope and summing over all photon energies, the response of each isotope can be calculated. These are then compared relative to the calculated response for Co-60 (+/- 1 standard deviation) in Table 5: Monte Carlo Estimate of Chamber Response Relative to Co-60, by Isotope

Table 5: Monte Carlo Estimate of Chamber Response Relative to Co-60, by Isotope

Isotope	Primary Energy (keV)	Response (pA/microCi)	+/-	Response relative to Co-60	+/-
In-111	23	5.36E-02	1.0E-03	4.36E-01	1.3E-02
I-125	27	6.15E-02	3.7E-04	5.01E-01	8.5E-03
Xe-133	30/80	3.41E-02	3.2E-04	2.78E-01	5.6E-03
Tl-201	70	2.90E-02	4.6E-04	2.37E-01	6.3E-03
Co-57	122	1.83E-02	4.1E-04	1.49E-01	5.0E-03
Tc-99m	140	1.60E-02	3.8E-04	1.30E-01	4.5E-03
Ga-67	93/184/300	1.87E-02	4.4E-04	1.52E-01	5.2E-03
Ba-133	30/80/355	9.46E-02	1.3E-03	7.71E-01	1.9E-02
I-131	364	2.70E-02	8.0E-04	2.20E-01	8.9E-03
F-18	511	5.92E-02	1.8E-03	4.82E-01	2.0E-02
Cs-137	661	3.59E-02	8.4E-04	2.92E-01	1.0E-02
Mo-99	740	3.54E-03	8.5E-05	2.89E-02	1.0E-03
Co-60	1173/1132	1.23E-01	1.3E-03	1.00E+00	N/A

A comparison of the relative responses from the Monte Carlo calculation with the measured values is shown in Table 6.

Table 6: Comparison of Monte Carlo (MC) Relative Response with Measured Relative Response

Isotope	Primary Energy (keV)	MC relative response	+/-	Measured relative response	+/-
In-111	23	0.436	0.013	0.388	0.009
I-125	27	0.501	0.008	0.462	0.012
Xe-133	30/80	0.278	0.006	0.277	0.003
Tl-201	70	0.237	0.006	0.244	0.005
Co-57	122	0.149	0.005	0.149	0.002
Tc-99m	140	0.130	0.005	0.137	0.002
Ga-67	93/184/300	0.152	0.005	0.156	0.003
Ba-133	30/80/355	0.771	0.019	0.712	0.015
I-131	364	0.220	0.009	0.224	0.001
F-18	511	0.482	0.020	0.542	0.026
Cs-137	661	0.292	0.010	0.295	0.004
Mo-99	740	0.029	0.001	0.027	0.000
Co-60	1173/1132	1.000	N/A	1.000	0.012

The relative response as predicted by the Monte Carlo simulation only matches the relative response measured for higher energy photons. Thus a correction to the low energy response is necessary in order to have the energy response curve match the measured response. This correction is applied only to the low energy photoelectric peak (photon energy less than 88 keV). A multiplicative correction factor was applied to the low energy photoelectric peak to reduce the magnitude of the peak. However this factor could not be simply multiplied by the response of all sections

of the peak, as the peak had to match the higher energy section adjacent to the low energy photoelectric peak. Instead the multiplicative factor was directly multiplied by the sections from 40 keV and below, and the section from 40 to 88 keV was multiplied by a factor which ran linearly from the full factor at 40 keV to a factor of unity at 88 keV. By iteratively attempting different values for the multiplicative factor, a value of 0.9 was arrived at as meeting the most isotopes.

Table 7: Comparison of Measured Response Relative to Co-60 with Modified and Unmodified Monte Carlo (MC) Calculations

Isotope	Measured	Unmodified MC	Modified MC
In-111	0.388	0.436	0.417
I-125	0.462	0.501	0.445
Xe-133	0.277	0.278	0.267
Tl-201	0.244	0.237	0.233
Co-57	0.149	0.149	0.154
Tc-99m	0.137	0.130	0.133
Ga-67	0.156	0.152	0.156
Ba-133	0.712	0.771	0.721
I-131	0.224	0.220	0.216
F-18	0.542	0.482	0.476
Cs-137	0.295	0.292	0.285
Mo-99	0.027	0.029	0.028
Co-60	1.000	1.000	1.000

The only isotope for which the value does not provide a good correction is Co-57. Co-57 is not a NIST calibrated isotope. Tc-99m, which has a very similar photon energy (140 keV vs. 122 & 136 keV for Co-57) is a NIST calibrated isotope for which the Monte Carlo response curve makes a correct prediction. This makes it appear likely that the calibration of the Co-57 source may be off by 3%. As a NIST traceable isotope, its calibration is specified to be within +/-5% of NIST standards. When this fact is taken into account, the multiplicative correction factor of 0.9 provides a better estimate of chamber response characteristics than the original Monte Carlo simulation.

The following figures show the improved ("modified Monte Carlo") chamber response curve, and a comparison between the unmodified and modified response curves:

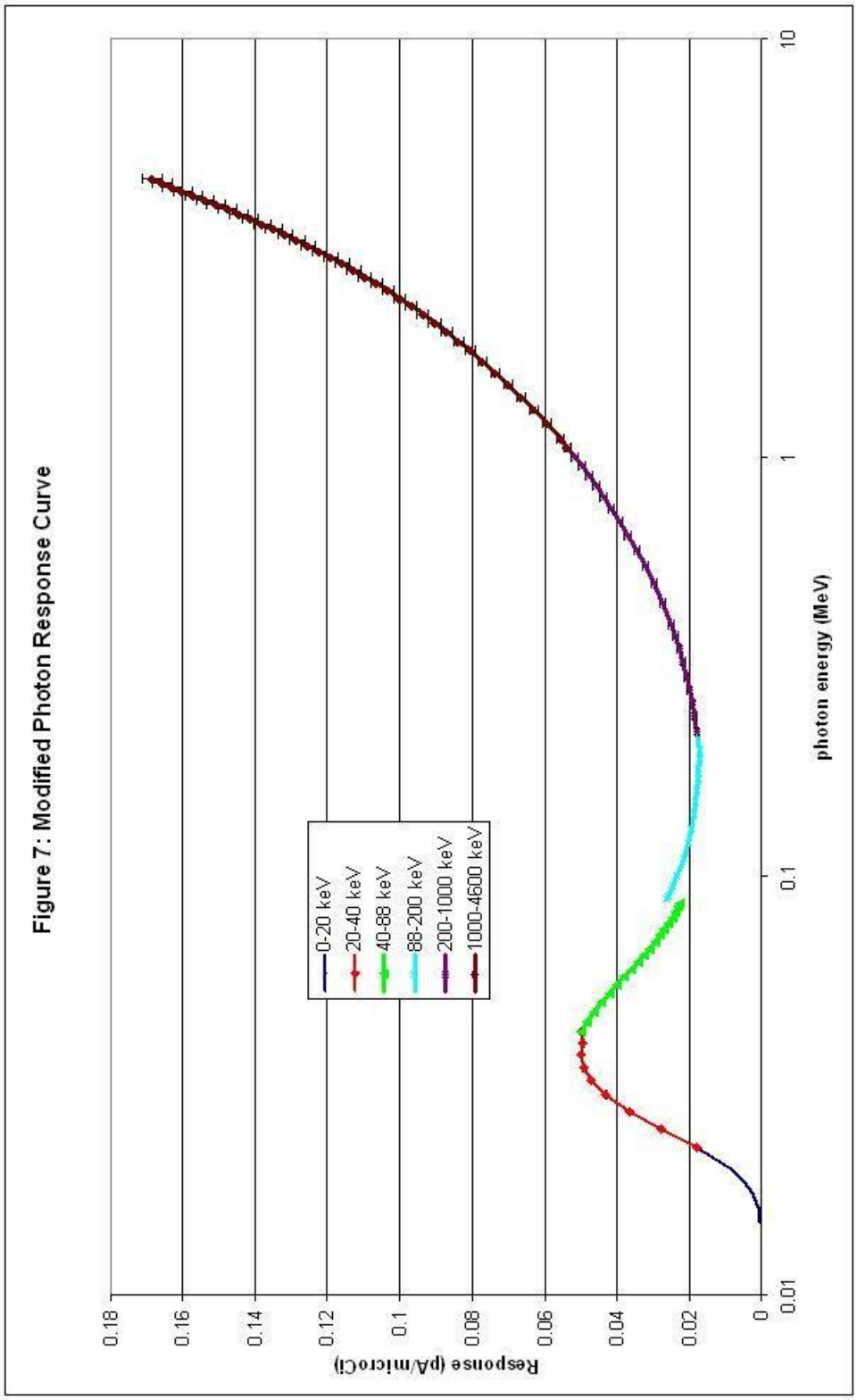
Figure 7: Modified Photon Response Curve
Response (pA/microCi)
0.18
0.16
0.14
0.12
0.1
0.08
0.06
0.04
0.02
0
0.01
0.1
1
10
photon energy (MeV)
0-20 keV
20-40 keV
40-88 keV
88-200 keV
200-1000 keV
1000-4600 keV

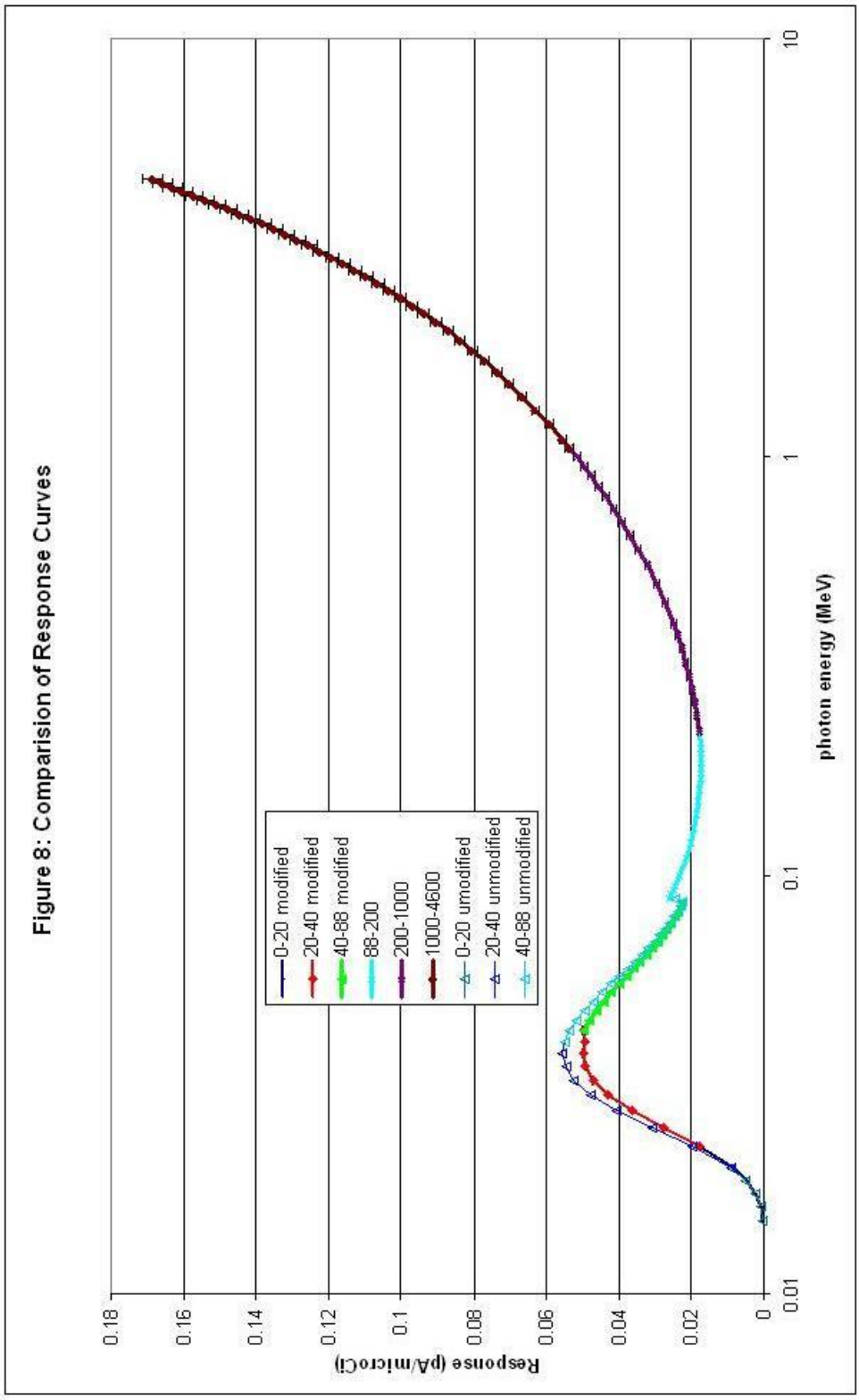
Figure 8: Comparision of Response Curves
Response (pA/microCi)
photon energy (MeV)
0-20 modified
20-40 modified
40-88 modified
88-200
200-1000
1000-4600
0-20 umodified
20-40 unmodified
40-88 unmodified
0.18
0.16
0.14
0.12
0.1
0.08
0.06
0.04
0.02
0
0.01
0.1
1
10

Conclusion

The response characteristics of the Atomlab Re-entrant Ionization Chamber have been measured for photons and positrons. Monte Carlo simulation of the chamber response is very close to the actual measured response for all but low energy (less than 88 keV) photons. A correction factor, empirically derived, can modify the Monte Carlo calculated photon response curve to match the actual measured one.

It is possible that Monte Carlo simulation of the photon response curve could be made to match the actual response curve at low energy. This would entail having more accurate knowledge of the thickness of the chamber's inner aluminum wall. Variations in this wall thickness between chamber batches manufactured on different dates are as large as the difference between the modified and unmodified Monte Carlo calculated curves. As highly precise wall thickness information may not be available for all chambers, the published energy response curve at low energies should be treated as an average value for all chambers, rather than the correct one for any individual chamber. Because additional correction factors usually need to be applied when measuring low energy isotopes, the variation from lack of knowledge of the exact wall thickness can be absorbed into these clinical correction factors.

References

1) Attix, Frank H., *Introduction to Radiological Physics and Radiation Dosimetry*, New York: John Wiley and Sons, Inc., 1986

2) Knoll, Glen F., *Radiation Detection and Measurement*, New York: John Wiley and Sons, Inc., 1979

3) Browne, Edgardo, and Richard B. Firestone, *Table of Radioactive Isotopes*, New York: John Wiley and Sons, Inc., 1986

4) National Nuclear Data Center, *Nudat 2.2 Database*, Upton, NY: Brookhaven National Laboratory, 2007

5) Baker, M. and M. J. Woods, "Intercomparison of ^{123}I Solution Sources in UK Hospitals, 2000", Teddington, UK: National Physical Laboratory, 2000

6) United States Pharmacopoeia National Formulary XXIII

7) Private Communication between William Simon and Michael Zimmer of Northwestern Memorial Hospital, 12/3/03

8) Suzuki, Arata, Marcia N. Suzuki, and Arthur M. Weis, "Analysis of a Radioisotope Calibrator." Journal of Nuclear Medicine Technology, Vol. 4 No. 4:193-198.

9) Rossi, Bruno B., and Hans H. Staub, *Ionization Chambers and Counters, Experimental Techniques,* New York: McGraw-Hill Book Company, Inc., 1949

10) Hubbell, J.H. and Seltzer, S.M. (2004), *Tables of X-Ray Mass Attenuation Coefficients and Mass Energy-Absorption Coefficients* (version 1.4). [Online] Available: http://physics.nist.gov/xaamdi [2007, March 20]. National Institute of Standards and Technology, Gaithersburg, MD. Originally published as NISTIR 5632, National Institute of Standards and Technology, Gaithersburg, MD (1995).

11) F. Salvat, J. M. Fernandez-Varea, E. Acosta, and J. Sempau, *PENELOPE – A Code System for Monte Carlo Simulation of Electron and Photon Transport* (OECD Nuclear Energy Agency, Issy-les-Moulineaux, France; 2001) NEA/NSC/DOC(2001)12, ISBN: 92-64-18475-9.

12) Chu, Robert Y.L. and William E. Simon, “Quality Control Testing of Dose Calibrators.” Journal of Nuclear Medicine Technology, 24:124-128 (1996)

13) Simon, William E., “Atomlab Dial Value Theory”, Sun Nuclear Corporation internal memo.

14) Siegel, Jeffrey A., Brian E. Zimmerman, Kory Kodimer, Mary A. Dell, and William E. Simon, “Accurate Dose Calibrator Activity Measurement of ^{90}Y-Ibritumamab Tiuxetan.” Journal of Nuclear Medicine Vol. 45 No. 3:450-454(2004)

15) W-M Yao et al J. Phys.G: Nucl. Part. Phys. Vol. 33 1 (2006)

16) D.W.O. Rogers, I. Kawrakow, N.V. Klassen, C.K. Ross, J.P. Seuntjens, K.R. Shortt, L. van der Zwan, J. Borg and G. Daskalov, “NRC Activities and Publications, 1997-1999 Report to CCRI(I) Meeting, BIPM May 26 -28 1999: Ionizing Radiation Standards”, Ottawa: National Research Council of Canada

Appendix

Tables

Table 8: Photons Emitted by Measured Isotopes (obtained from references 3 and 4).

Isotope	Energy (keV)	Probability
Co-60	1173.2	0.999
	1332.5	0.9998

Isotope	Energy (keV)	Probability
Co-57	122.06065	0.856
	136.47356	0.1068
	230.4	0.000004
	339.69	0.000037
	352.33	0.00003
	366.8	0.000012
	570.09	0.000158
	692.41	0.00149
	706.54	0.00005

Isotope	Energy (keV)	Probability
Ga-67	91.266	0.0316
	93.311	0.392
	184.577	0.212
	208.951	0.024
	300.219	0.168
	393.529	0.0468
	494.169	0.000691
	703.11	0.000106
	794.386	0.00054
	887.693	0.00149

Isotope	Energy (keV)	Probability
Tc(m)-99	18.251	0.0214
	18.367	0.0407
	20.599	0.0033
	20.619	0.00639
	21.005	0.00145
	140.511	0.87
	142.63	0.000187

Isotope	Energy (keV)	Probability
Mo-99	242.29	0.000025
	249.03	0.000039
	366.421	0.01191
	380.13	0.000104
	391.7	0.000032
	410.27	0.000019
	411.491	0.000146
	457.6	0.000081
	469.63	0.000027
	528.788	0.00057
	537.79	0.000033
	580.51	0.000032
	620.03	0.000023
	621.771	0.00018
	689.6	4.2E-06
	739.5	0.1213
	761.77	0.000004
	777.921	0.0426
	822.972	0.00133
	861.2	0.00007
	960.754	0.00095
	986.44	0.000015
	1001.343	0.000055
	1017	6.1E-06
	1056.2	1.08E-05

Isotope	Energy (keV)	Probability
In-111	22.984	0.241
	23.174	0.453
	26.06	0.0392
	26.095	0.0755
	26.644	0.0194
	150.81	0.00003
	171.28	0.907
	245.35	0.941

Isotope	Energy (keV)	Probability
I-125	27.202	0.401
	27.472	0.74
	30.944	0.0683
	30.995	0.132
	31.704	0.038
	35.4922	0.0668

Isotope	Energy (keV)	Probability
I-131	29.461	0.0138
	29.782	0.0254
	33.562	0.00238
	33.624	0.00459
	34.419	0.00139
	80.185	0.0262
	85.9	9E-07
	177.214	0.0027
	232.18	0.000032
	272.498	0.000578
	284.305	0.0614
	295.8	0.000018
	302.4	0.000047
	318.088	0.000776
	324.651	0.000212
	325.789	0.00274
	358.4	0.00016
	364.489	0.817
	404.814	0.000547
	503.004	0.0036
	636.989	0.0717
	642.719	0.00217
	722.911	0.0177

Isotope	Energy (keV)	Probability
Ba-133	30.625	0.356
	30.973	0.657
	34.967	0.18
	36.006	0.0439
	53.148	0.0217
	79.612	0.0318
	80.989	0.342
	160.601	0.006
	223.24	0.0046
	276.388	0.0709
	302.851	0.184
	355.999	0.622
	383.841	0.0892

Isotope	Energy (keV)	Probability
Xe-133	30.625	0.142
	30.973	0.259
	34.92	0.0245
	34.987	0.0474
	35.818	0.0147
	79.623	0.0027
	80.997	0.38
	160.613	0.00066
	223.234	1.2E-06
	302.853	0.000048
	383.851	0.000024

Isotope	Energy (keV)	Probability
Cs-137	31.817	0.0205
	32.194	0.0377
	36.304	0.00342
	36.378	0.0066
	37.255	0.00264
	283.5	5.8E-06
	661.657	0.8521

Isotope	Energy (keV)	Probability
Tl-201	26.34	0.000086
	30.6	0.00253
	32.19	0.00258
	68.894	0.268
	70.818	0.451
	79.824	0.0544
	80.225	0.104
	82.473	0.0377
	135.34	0.02565
	141.1	0.000063
	165.88	0.00155
	167.43	0.1

Table 9: Positron Energies Emitted from F-18

Isotope	Positron Energy (keV)	Probability
F-18	15.85	0.017989
	47.5	0.044026
	79.15	0.060184
	110.85	0.071027
	142.55	0.077991
	174.2	0.081809
	205.85	0.082891
	237.55	0.081663
	269.25	0.07831
	300.9	0.073191
	332.55	0.06659
	364.25	0.058868
	395.95	0.050267
	427.6	0.041187
	459.25	0.032062
	490.95	0.023218
	522.65	0.015151
	554.3	0.008372
	585.95	0.003219
	617.65	0.000589

Table 10: Monte Carlo Photon Response Curve Polynomial Expansion Coefficients

Photon Energy (keV)	5th order	4th order	3rd order	2nd order	1st order	zeroth order
0-20	0.00 E+00	0.00 E+00	0.00 E+00	3.29 E+02	-9.72 E+00	7.21 E-02
20-40	-2.43 E+07	4.21 E+06	-2.85 E+05	9.24 E+03	-1.40 E+02	7.88 E-01
40-88	3.08 E+05	-1.07 E+05	1.48 E+04	-1.00 E+03	3.22 E+01	-3.34 E-01
88-200	0.00 E+00	8.32 E+01	-5.71 E+01	1.51 E+01	-1.81 E+00	1.02 E-01
200-1000	0.00 E+00	5.71 E-02	-1.70 E-01	1.72 E-01	-2.44 E-02	1.66 E-02
1000-4600	-8.38 E-05	8.76 E-04	-2.66 E-03	-2.12 E-04	4.41 E-02	9.79 E-03

Table 11: Modified Monte Carlo Photon Response Curve Polynomial Expansion Coefficients

Photon Energy (keV)	5th order	4th order	3rd order	2nd order	1st order	zeroth order
0-20	0.00 E+00	0.00 E+00	0.00 E+00	2.96 E+02	-8.75 E+00	6.49 E-02
20-40	-2.18 E+07	3.79 E+06	-2.56 E+05	8.32 E+03	-1.26 E+02	7.09 E-01
40-88	2.82 E+05	-9.83 E+04	1.36 E+04	-9.24 E+02	2.99 E+01	-3.15 E-01
88-200	-5.13 E+01	1.29 E+02	-7.34 E+01	1.80 E+01	-2.10 E+00	1.14 E-01
200-1000	0.00 E+00	5.71 E-02	-1.70 E-01	1.72 E-01	-2.44 E-02	1.66 E-02
1000-4600	-8.38 E-05	8.76 E-04	-2.66 E-03	-2.12 E-04	4.41 E-02	9.79 E-03

Photographs

Photograph 1: Atomlab 200's

This photo shows the older 90 psia style of Atomlab chambers, manufactured from 1991-2007 and sold under the Biodex label. Each chamber requires a separate controller.

Photograph 2: Atomlab 500's

This photo shows the newer 38 psia style of Atomlab chambers. One Atomlab 500 controller is capable of displaying from any of the four chambers connected to it. Note the chamber with the lead cover removed.